

Syngas Formation by Microwave-induced Co–Mo and Ni–Mo Catalysts

Chih Ju G. Jou^{1*} and Chien Li Lee²

¹Department of Safety, Health and Environmental Engineering, National Kaohsiung University of Science and Technology, 2, Juoyue Rd., Nantz District, Kaohsiung 811, Taiwan

²Research and Development Center for Water Resource and Conservation, National Kaohsiung University of Science and Technology, 2, Juoyue Rd., Nantz District, Kaohsiung 811, Taiwan

(Received April 1, 2024; accepted June 11, 2024)

Keywords: Ni–Mo catalyst, Co–Mo catalyst, syngas, microwave

In this study, the microwave-induced Co–Mo and Ni–Mo catalysts were combined with a high-dielectric-constant medium to absorb microwave energy and convert it into the heat energy required for syngas production. The microwave conditions were a microwave power of 450 W and a total microwave time of 210 min with the volume ratios $\text{CH}_4/\text{air} = 1:2$ (partial oxidation) and $\text{CH}_4/\text{CO}_2 = 2:1$ (dry reforming reaction). The results showed that the average yields of H_2 and CO were 43 and 35.7% in the partial oxidation reaction with Ni–Mo as catalyst, whereas those in the dry reforming reaction were 44.4 and 24.9%, respectively. On the other hand, with Co–Mo as the catalyst, the average yields of H_2 and CO were 50.7 and 35.9% in the partial oxidation reaction, whereas those in the dry reforming reaction were 62.6 and 40.6%, respectively. Owing to the high activity of the Ni–Mo catalyst, it is easier to shield the metal coated on the surface by coke deposition. As the reaction time proceeds, the activity of the Ni–Mo catalyst decreases, and the syngas yield is reduced. Therefore, it is feasible and innovative to combine microwave-induced Ni–Mo and Co–Mo catalysts with a high-dielectric-constant medium to absorb and convert microwave energy into heat energy to produce syngas.

1. Introduction

With the growth of the world's population and economic development, traditional fossil fuels such as coal, oil, and natural gas have become the backbone for meeting the global energy demand. However, upon combustion, these fossil fuels emit a large amount of greenhouse gases (GHG) (CO_2 and CH_4), leading to global warming, adverse effects on biodiversity, and extreme natural events such as floods and droughts.^(1,2) One important method of reducing CH_4 and CO_2 gases is to convert them into syngas, which is a valuable intermediate raw material for the synthesis of liquid fuels.⁽³⁾

Syngas is a mixture of CO and H_2 and is an important raw material for the chemical industry. Currently, there are three main methods of producing syngas from CH_4 : steam reforming, dry reforming, and catalytic partial oxidation. Compared with the first two methods, catalytic partial

*Corresponding author: e-mail: george@nkust.edu.tw
<https://doi.org/10.18494/SAM5053>

oxidation has several advantages: (1) It is a mild exothermic reaction that does not require high operating pressures,⁽⁴⁾ making it energy-efficient in terms of industrial process investment. (2) The H₂/CO molar ratio is close to 2, which is an ideal ratio for Fischer–Tropsch reactions and for synthesizing valuable intermediate raw materials such as methanol.^(4,5) (3) Catalytic partial oxidation can be applied under very high gas space velocity conditions, allowing for less investment in scale to produce larger capacities.^(6,7) The dry reforming of methane is a promising method for the transformation of the global energy industry towards low-emission and zero-emission fuels, reducing GHG emissions. It can simultaneously utilize CH₄ and CO₂ and convert them into high-value H₂ and CO syngas, which can be used as feedstock for the downstream synthesis of long-chain hydrocarbons or oxygenated compounds.⁽⁸⁾ The H₂/CO molar ratio varies depending on the catalyst used in catalytic partial oxidation. The rate-limiting step of most catalyst oxidation reactions changes with temperature and composition, and short contact time reactions have high methane conversion rates and syngas selectivity.^(9,10) For example, in a Pt/Al₂O₃ monolithic reactor operated at millisecond contact time, the methane conversion rate exceeds 60%, with CO and H₂ selectivities greater than 80 and 50%, respectively. Ni-based catalysts may result in higher syngas yields, but they require operation at low temperatures to minimize metal losses. On the other hand, Pt-based catalysts exhibit very stable characteristics, but with low H₂ selectivity.⁽¹¹⁾

The catalytic activity order for methane is as follows: Rh > Ni > Co > Pt > Fe > Mo > Pd. Ni-based catalysts can reduce metal losses when operated at low temperatures. The dispersion of the catalyst support is the main factor affecting catalytic activity, with higher dispersion leading to higher performance. The order of dispersion is Ni/Al₂O₃ > Ni/ZrO₂ > Ni/CeO₂, with Al₂O₃ as the carrier exhibiting high catalytic performance and achieving a methane selectivity of 94.5%.⁽¹²⁾ In a study by Peymani *et al.*, 10% Ni/CeO₂ catalyst was used for methane partial oxidation at a reaction temperature of 600 °C, a CH₄/O₂ feed volume ratio of 2:1, and a space velocity ranging from 22500 to 175500 mol/(gcat.h).⁽¹²⁾ The methane conversion rate increased from 60.95 to 76.73% with the space velocity. However, at higher space velocities, some reactions may be limited from a reaction kinetics perspective owing to increased heat release in the catalyst bed. When the feed ratio was changed to CH₄/air = 4:3, the CH₄ conversion rate increased to 92% owing to the increased O₂ content in the feed, promoting both partial and complete oxidations. Additionally, the selectivities of CO and H₂ decreased because complete oxidation occurred instead of partial oxidation as the oxygen content increased. Therefore, with changes in feed ratio, combustion reactions became more favorable than partial oxidation, resulting in increased CO₂ and H₂O contents and decreased selectivities of CO and H₂.⁽¹³⁾

In a study by Lo *et al.*, Ni and Fe catalysts were used as partial oxidation catalysts. When the CH₄/air feed volume ratio was 1:1, higher H₂ and CO yields were obtained with the Ni catalyst than with the Fe catalyst (54.7 vs 46.0% for H₂ and 19.7 vs 14.4% for CO).⁽¹⁴⁾ In another study by Lo *et al.* using the platinum/palladium/rhodium (Pt/Pd/Rh) spent catalyst supported on MgO–Al₂O₃–SiO₂ as the main carrier, in the methane partial oxidation process, when the CH₄/air feed volume ratio was 1:2, the yields were 67.3% for H₂ and 11.6% for CO.⁽¹⁵⁾

In this study, Co–Mo and Ni–Mo catalysts were combined with activated carbon under microwave energy conditions. The high dielectric constant of activated carbon allows it to

absorb microwave energy and convert it into heat energy, providing the required energy for methane dry reforming (CH_4 and CO_2) to produce syngas. Dry reforming converts CH_4 and CO_2 into a high-value synthesis gas consisting of H_2 and CO . This process holds great promise for the current global energy industry's transition towards low-emission and zero-emission fuel development, aiming to reduce GHG emissions.

2. Experimental Equipment and Methods

2.1 Experimental equipment

A microwave oven (SAMPO, MOB-P23) equipped with proportional-integral and derivative control for adjusting the output power was used. The microwave frequency was 2.45 GHz and the maximum output power was 850 W. The reactor consists of a main body connected to a thin tube, allowing the direct introduction of gas into a customized 80 ml quartz glass material. The microholes at the bottom of the reactor (1 mm diameter, 40 microholes) are designed for gas ventilation. The experimental setup is shown in Fig. 1.

In this study, Co–Mo and Ni–Mo solid catalysts with Al_2O_3 as the carrier, which are commonly used in the petrochemical industry, were selected. Microwave induction and a high-dielectric-constant carbon medium were used to absorb microwaves and provide the energy required for syngas production.

2.2 Experimental methods

Before placing 6 g of the catalyst into the reaction bottle, insulation cotton and 1 g of medium activated carbon were placed at the bottom of the reaction bottle. The experimental conditions were as follows: (1) CH_4 + air and CH_4 + CO_2 . The gases under the two feed conditions were introduced into the reaction bottle through the gas mixing chamber. (2) The CH_4 /air volume flow ratio changed from 10/10 (1:1) to 10/20 (1:2) and 20/10 (2:1) (mL/min). The bulk temperature of the catalyst was increased in the microwave to approximately 450 °C (which took 60 min). Sampling was performed using a 1 ml gas-tight syringe and subsequently every 60 min. The

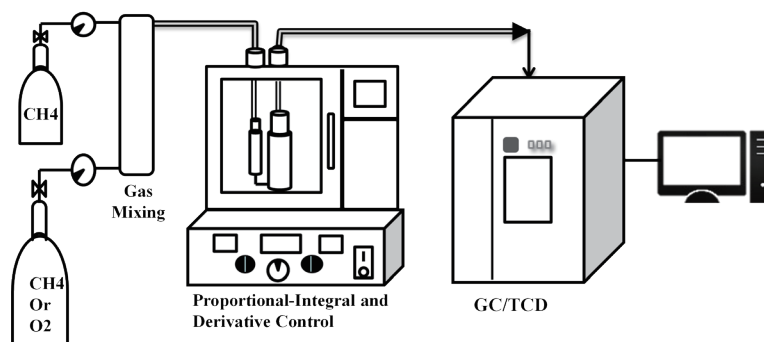


Fig. 1. Schematic of the experimental setup and process.

total microwave time was 240 min. The collected gas samples were injected into a gas chromatography-thermal conductivity detector (GC/TCD) for the quantitative analyses of the products to determine the final products and their yields. The syngas yield was then calculated on the basis of the carbon mass to establish a mass balance.

2.3 Analyses

Chemical composition analyses of organic intermediates and final products were performed with a GC-TCD (SHIMADZU GC-2014). A tail gas sample (1 μ L) was taken every 30 min with three replicates for the measurements of CO, CO₂, H₂, and CH₄. On the other hand, a carbon determinator (Eltra, CS 800) was used to analyze the coke content of the catalyst. The images produced by a scanning electron microscope (SEM) (Hitachi, SU8000) were used to observe the surface structure of the catalyst.

3. Results and Discussion

3.1 Effects of Co–Mo and Ni–Mo catalysts on the production of syngas at different CH₄/air volume flow ratios

The partial oxidation reaction of methane is divided into two mechanisms: the direct mechanism, where methane reacts with oxygen on the catalyst surface to undergo partial oxidation and directly produce H₂ and CO ($\text{CH}_4 + 0.5\text{O}_2 \rightarrow \text{CO} + 2\text{H}_2$), and the indirect mechanism, where methane first undergoes complete oxidation to produce H₂O and CO₂ ($\text{CH}_4 + \text{O}_2 \rightarrow \text{H}_2\text{O} + \text{CO}_2$), and the remaining methane reacts with water through steam reforming ($\text{CH}_4 + \text{H}_2\text{O} \rightarrow \text{CO} + 3\text{H}_2$) and with carbon dioxide through dry reforming ($\text{CH}_4 + \text{CO}_2 \rightarrow 2\text{CO} + 2\text{H}_2$).⁽¹⁶⁾ The conditions that determine the two reaction pathways are primarily temperature and the effective contact time between the catalyst and the gas. Direct partial oxidation reactions require a reaction temperature above 750 °C and a contact time of less than 0.1 s on the catalyst surface.⁽¹⁷⁾

The methane partial oxidation reaction mechanism relies on the heat generated from complete oxidation reactions to proceed with subsequent reactions. Therefore, the feed ratio plays a crucial role in the production of synthesis gas. Co–Mo catalysts with added activity were used as the medium, and the CH₄/air volume flow ratio was adjusted to 1:1, 1:2, and 2:1. A microwave power of 450 W was utilized, along with a total irradiation time of 240 min. The results depicted in Fig. 2 demonstrate that the average hydrogen yields for CH₄/air volume flow ratios of 1:1, 1:2, and 2:1 are 64.6, 55.1, and 58.1%, respectively. Furthermore, Fig. 3 reveals that the average carbon monoxide yields are 29.9, 36.9, and 22.7%, respectively. When the air proportion in the feed is higher, an increase in oxygen content leads to decreases in the selectivities of hydrogen and carbon monoxide. The added activated carbon reacts with oxygen, resulting in an upward trend in carbon monoxide yield. On the other hand, under conditions where the methane proportion in the feed is higher, after methane undergoes complete oxidation and reacts with water and carbon dioxide through reforming reactions, a fraction of the remaining methane undergoes cracking

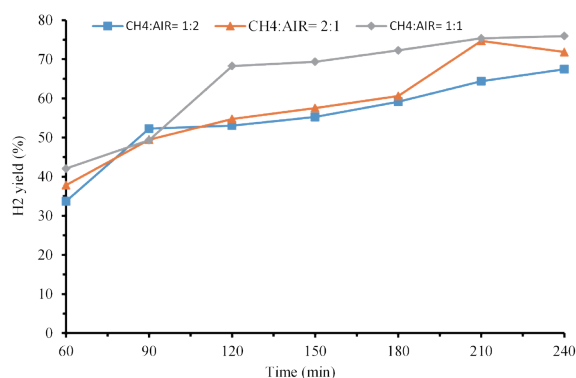


Fig. 2. (Color online) H₂ yields of the Co–Mo catalyst under different CH₄/air volume flow ratios.

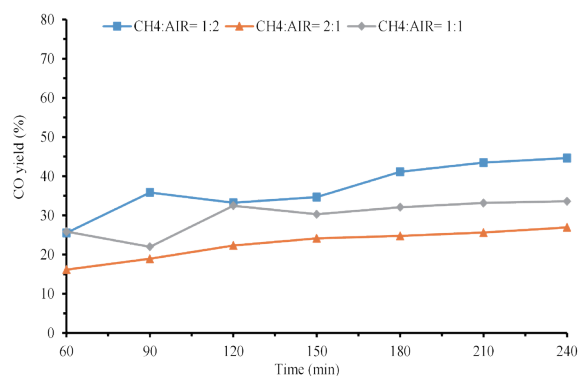


Fig. 3. (Color online) CO yields of the Co–Mo catalyst under different CH₄/air volume flow ratios.

reactions to produce carbon and hydrogen. As a result, there is a decrease in carbon monoxide yield.

Owing to the high activity of the Ni–Mo catalyst, it is easier to shield the metal coated on the surface by coke deposition. As the reaction time proceeds, the activity of the Ni–Mo catalyst, as well as the yield of syngas, decreases. Under the same conditions (CH₄/air volume flow ratios of 1:1, 1:2, and 2:1, microwave power of 450 W, and total microwave time of 240 min), the results shown in Fig. 4 indicate that the average hydrogen yields are 38.3, 22.2, and 43.1%, respectively. When the CH₄/air influent volumetric ratio is 1:2, a lower ratio of methane would decrease the rate of recombination reaction with H₂O and CO₂, resulting in a reduction of H₂. Similarly, the results shown in Fig. 5 reveal that the average carbon monoxide yields are 26.8, 23.8, and 23.6%, respectively.

3.2 Effects of Co–Mo and Ni–Mo catalysts on the production of syngas at different CH₄/CO₂ volume flow ratios

The methane (CH₃-H) bond dissociation energy is 435 kJ/mol, whereas the carbon dioxide (CO-O) bond dissociation energy is 526 kJ/mol. This indicates that the overall reaction requires high temperature to achieve the equilibrium conversion of syngas.⁽¹⁸⁾ The dry reforming reaction mechanism involves a single-function mechanism, where methane and carbon dioxide are adsorbed and dissociated by active metals. Methane dissociation produces hydrogen and hydrocarbon compounds, whereas carbon dioxide dissociation produces oxygen and carbon monoxide. However, the dehydrogenated carbonaceous species deposit on the metal surface, hindering the adsorption and dissociation of carbon dioxide, leading to catalyst deactivation due to coke deposition. Another mechanism is the dual-function mechanism, where methane is adsorbed and reacts on the metal surface, whereas carbon dioxide is adsorbed and reacts on the catalyst support surface. The products of methane and carbon dioxide dissociation react at the metal-support interface, resulting in the formation of syngas.⁽¹⁹⁾ The factors that affect both mechanisms include the active metal, catalyst support, and temperature. Regardless of the mechanism, the reforming reaction of methane and carbon dioxide tends to favor the low-energy

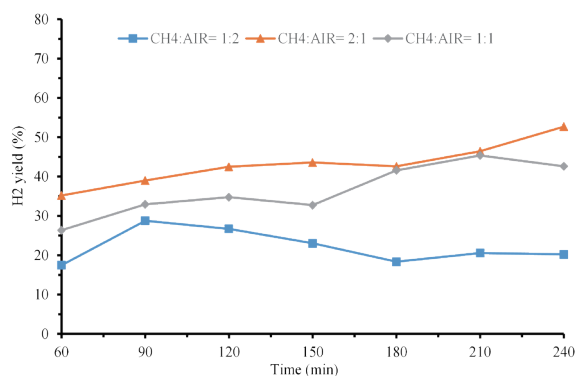


Fig. 4. (Color online) H₂ yields of the Ni–Mo catalyst under different CH₄/air volume flow ratios.

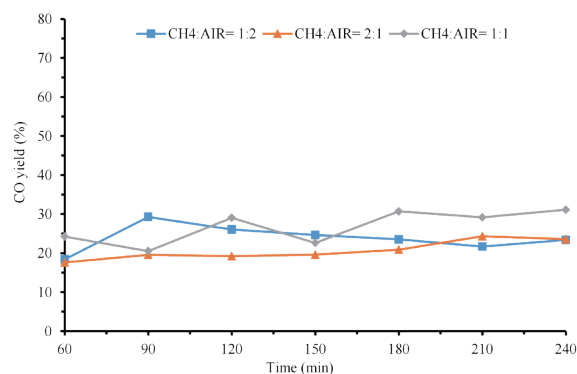


Fig. 5. (Color online) CO yields of the Ni–Mo catalyst under different CH₄/air volume flow ratios.

decomposition pathways, such as methane cracking ($\text{CH}_4 \rightarrow \text{C(s)} + 2\text{H}_2$) and carbon gasification ($\text{C(s)} + \text{CO}_2 \rightarrow 2\text{CO}$) reactions.

Under different feed ratios, a higher proportion of carbon dioxide in the feed will increase carbon monoxide production and decrease hydrogen production. On the other hand, a higher proportion of methane in the feed will increase hydrogen production and decrease carbon monoxide production owing to excess methane undergoing cracking reactions to produce carbon and hydrogen. With the Co–Mo catalyst and an active medium, a microwave power of 450 W, and a total irradiation time of 240 min, the results in Fig. 6 show that the average hydrogen yields were 24.6, 18.7, and 43.6% for CH₄/CO₂ volume flow ratios of 1:1, 1:2, and 2:1, respectively. Figure 7 shows that the average CO yields were 30.1, 26.4, and 30.4%, respectively.

Ni catalysts exhibit high activity for methane cracking reactions, leading to the formation of carbon, which can easily deposit on the catalyst surface and affect the reaction. Therefore, in dry reforming reactions for syngas production, Ni–Mo catalysts only show a slight improvement in yield. Under the same conditions (CH₄/CO₂ volume flow ratios of 1:1, 1:2, and 2:1, microwave power of 450 W, and total irradiation time of 240 min), the results in Fig. 8 show that the average hydrogen yields were 23.2, 20.6, and 51.8%, respectively. Figure 9 shows that the average CO yields were 24.1, 27.3, and 26.2%, respectively.

3.3 Carbon content and surface structure analyses of Co–Mo and Ni–Mo catalysts after microwave reactions

Factors that affect the carbon deposition morphology on catalyst surfaces include temperature and the types of metals and support used. When the catalyst support is Al₂O₃, which has a high oxygen storage capacity, it interacts with the active metals to enhance the mobility of oxygen atoms through the lattice. This facilitates the generation of oxygen vacancies for CO₂ adsorption, inhibits coke formation, and prevents metal particle sintering.⁽²⁰⁾ The acidity of the active metal, such as Ni, promotes coke formation, whereas the higher alkalinity of the active metal, such as Mo, favors CO₂ adsorption and a better suppression of coke formation, leading to a higher utilization of surface oxygen.⁽¹⁸⁾ As the reaction temperature increases, the carbon deposition

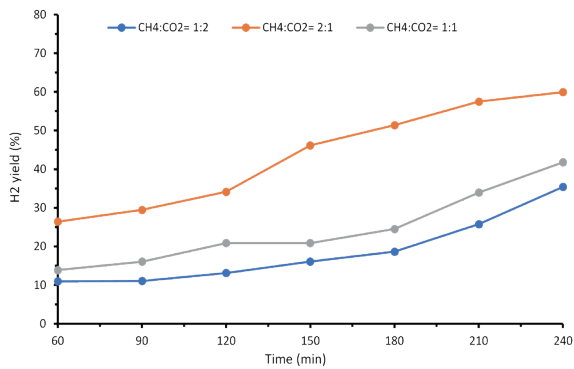


Fig. 6. (Color online) H₂ yields of the Co–Mo catalyst under different CH₄/CO₂ volume flow ratios.

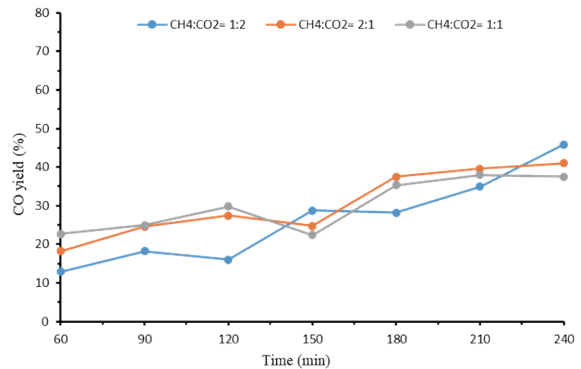


Fig. 7. (Color online) CO yields of the Co–Mo catalyst under different CH₄/CO₂ volume flow ratios.

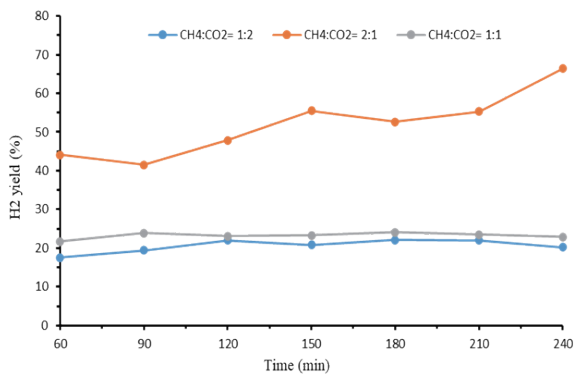


Fig. 8. (Color online) H₂ yields of the Ni–Mo catalyst under different CH₄/CO₂ volume flow ratios.

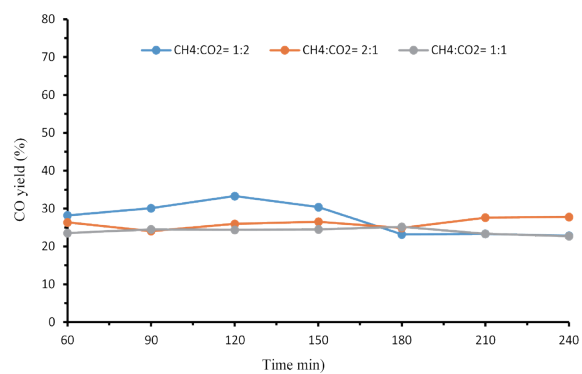


Fig. 9. (Color online) CO yields of the Ni–Mo catalyst under different CH₄/CO₂ volume flow ratios.

morphology changes, with an accelerated rate of coke formation and an increase in filamentous carbon formation.⁽¹²⁾

Figures 10(a) and 10(b) show the surface structures of the Co–Mo catalyst obtained before and after microwave treatment. Figure 10(b) shows that the amount of coke formed on the Co–Mo catalyst after microwave treatment increased (9.5 wt.%), resulting in a smoother catalyst surface appearance. Figures 11(a) and 11(b) show the surface structures of the Ni–Mo catalyst obtained before and after microwave treatment. Figure 11(b) shows that the amount of coke formed on the Ni–Mo catalyst increased after microwave treatment (9.9 wt.%), because the high activity of the Ni metal and the high reaction temperature increase the rate of coke formation. The coke forms on the catalyst surface in a filamentous form.

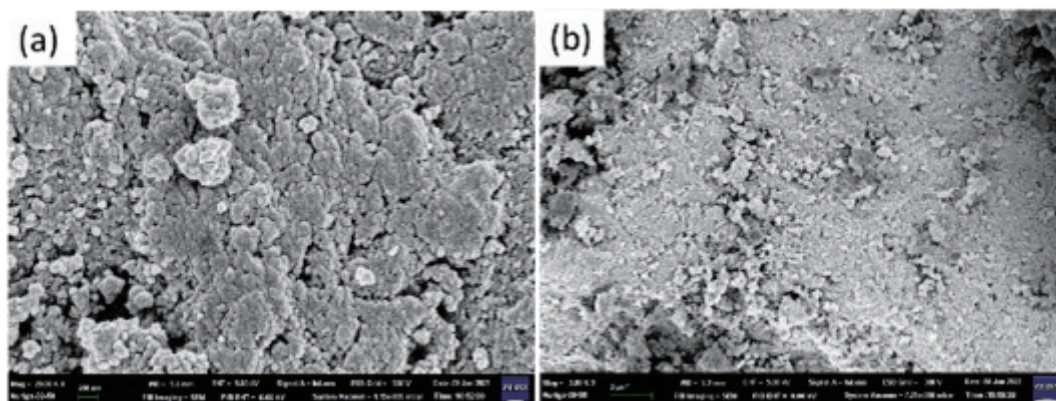


Fig. 10. SEM images obtained before and after Co–Mo catalyst reaction.

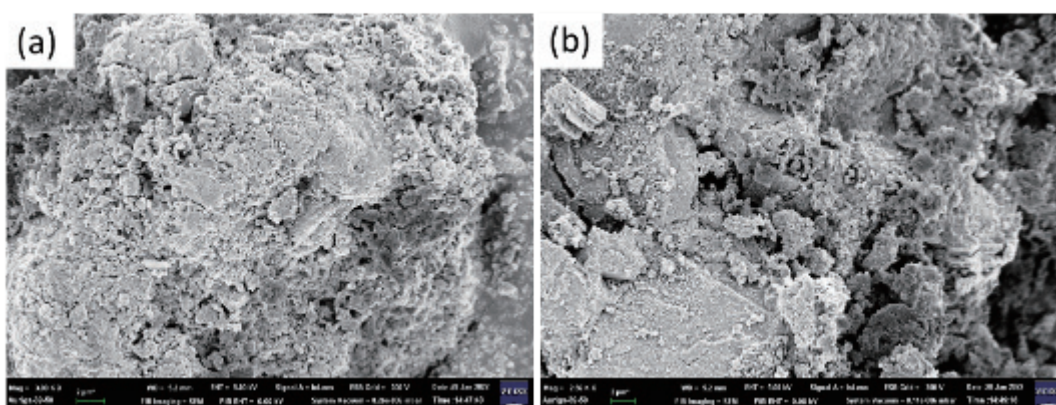


Fig. 11. SEM images obtained before and after Ni–Mo catalyst reaction.

4. Conclusions

In this study, Co–Mo and Ni–Mo were used as catalysts to produce syngas, with activated carbon added as the microwave medium. Activated carbon under microwave treatment absorbs and converts microwave energy into heat energy to provide the energy required for syngas production. Under the same microwave conditions (microwave power of 450 W, total microwave time of 240 min, and volume flow ratios of $\text{CH}_4/\text{air} = 1:2$ and $\text{CH}_4/\text{CO}_2 = 2:1$), the results showed that, using the Co–Mo/C catalyst for the CH_4/air volume flow ratio of 1:2, the average yields of H_2 and CO were 50.7 and 35.9%, respectively. For the feed ratio of 2:1, the average yields of H_2 and CO were 62.6 and 40.6%, respectively. Using the Ni–Mo catalyst for the CH_4/air volume flow ratio of 1:2, the average yields of H_2 and CO were 43 and 35.7%, respectively. For the volume flow ratio of 2:1, the average yields of H_2 and CO were 44.4 and 24.9%, respectively. Owing to the high activity of the Ni metal in the Ni–Mo catalyst, the high reaction temperature speeds up the formation of coke, reducing the contact area of the metal and gradually reducing the activity of the Ni–Mo catalyst. Therefore, the yield of syngas decreases.

References

1. S. M. W. U. Hasnain, A. S. Farooqi, B. V. Ayodele, A. S. Farooqi, K. Sanaullah, and B. Abdullah: *J. Cleaner Prod.* **434** (2024) 139904. <https://doi.org/10.1016/j.jclepro.2023.139904>
2. C. Kou, S. Jia, Y. Luo, and X. Yuan: *Fuel* **324** (2022) 124401. <https://doi.org/10.1016/j.fuel.2022.124401>
3. M. Boscherini, A. Storione, M. Minelli, F. Miccio, and F. Doghieri: *Energies* **16** (2023) 6375. <https://doi.org/10.3390/en16176375>
4. M. Peymani, S. M. Alavi, and M. Rezaei: *Int. J. Hydrogen Energy* **41** (2016) 19057. <https://doi.org/10.1016/j.ijhydene.2016.07.072>
5. S. Pruksawan, B. Kitiyanan, and R. M. Ziff: *Chem. Eng. Sci.* **147** (2016) 128. <https://doi.org/10.1016/j.ces.2016.03.012>
6. M. Khajenoori, M. Rezaei, and B. Nematollahi: *J. Ind. Eng. Chem.* **19** (2013) 981. <https://doi.org/10.1016/j.jicc.2012.11.020>
7. J. Xu, W. Wei, A. Tian, Y. Fan, X. Bao, and C. Yu: *Catal. Today* **149** (2010) 191. <https://doi.org/10.1016/j.cattod.2009.07.087>
8. J. Tang, J. Meng, W. Pan, T. Gu, Q. Zhang, J. Zhang, X. Wang, C. Bu, and G. Piao: *Int. J. Hydrogen Energy* **48** (2023) 19033. <https://doi.org/10.1016/j.ijhydene.2023.01.370>
9. M. Peymani, S. M. Alavi, and M. Rezaei: *Int. J. Hydrogen Energy* **41** (2016) 6316. <https://doi.org/10.1016/j.ijhydene.2016.03.033>
10. J. A. Velasco, C. Fernandez, L. Lopez, S. Cabrera, M. Boutonnet, and S. Järås: *Fuel* **153** (2015) 192. <https://doi.org/10.1016/j.fuel.2015.03.009>
11. M. Das and W. J. Koros: *J. Membr. Sci.* **365** (2010) 399. <https://doi.org/10.1016/j.memsci.2010.09.029>
12. M. Peymani, S. M. Alavi, and M. Rezaei: *Appl. Catal., A* **529** (2017) 1. <https://doi.org/10.1016/j.apcata.2016.10.012>
13. Y. Liu, L. Zhu, X. Wang, S. Yin, F. Leng, F. Zhang, H. Lin, and S. Wang: *Chin. J. Chem. Eng.* **25** (2017) 602. <https://doi.org/10.1016/j.cjche.2016.10.019>
14. C. C. Lo, C. L. Lee, and C. J. G. Jou: *Sens. Mater.* **32** (2020) 283. <https://doi.org/10.18494/SAM.2020.2580>
15. C. C. Lo, C. L. Lee, T. Y. Tsai, and C. J. G. Jou: *Sens. Mater.* **32** (2020) 275. <https://doi.org/10.18494/SAM.2020.2579>
16. C. Alvarez-Galvan, M. Melian, L. Ruiz-Matas, J. L. Eslava, R. M. Navarro, M. Ahmadi, B. R. Cuenya, and J. L. G. Fierro: *Front. Chem.* **7** (2019) 104. <https://doi.org/10.3389/fchem.2019.00104>
17. A. Moral, I. Reyero, J. Llorca, F. Bimbela, and L. M. Gandía: *Catal. Today* **333** (2019) 259. <https://doi.org/10.1016/j.cattod.2018.04.003>
18. A. M. Ranjekar and G. D. Yadav: *J. Indian Chem. Soc.* **98** (2021) 100002. <https://doi.org/10.1016/j.jics.2021.100002>
19. P. Ferreira-Aparicio, I. Rodríguez-Ramos, J. A. Anderson, and A. Guerrero-Ruiz: *Appl. Catal. A* **202** (2000) 183. [https://doi.org/10.1016/S0926-860X\(00\)00525-1](https://doi.org/10.1016/S0926-860X(00)00525-1)
20. A. W. Budiman, S. H. Song, T. S. Chang, C. H. Shin, and M. J. Choi: *Catal. Surv. Asia* **16** (2012) 183. <https://doi.org/10.1007/s10563-012-9143-2>